Tuning size and seed position in small silver nanorods

Tuning Size and Seed Position in Small Silver Nanorods

Ana Sánchez-Iglesias[1,2], Xiaolu Zhuo[1], Wiebke Albrecht[3], Sara Bals[3], Luis M. Liz-Marzán[1,2,4,*]

[1] CIC biomaGUNE, Basque Research and Technology Alliance (BRTA), Paseo de Miramón 182, 20014 Donostia – San Sebastián, Spain

[2] Centro de Investigación Biomédica en Red, Bioingeniería, Biomateriales y Nanomedicina (CIBER-BBN), Paseo de Miramón 182, 20014 Donostia – San Sebastián, Spain

[3] EMAT and NANOlab Center of Excellence, University of Antwerp, Groenenborgerlaan 171, 2020 Antwerp, Belgium

[4] Ikerbasque, Basque Foundation for Science, 48013 Bilbao, Spain

ABSTRACT: Although high-quality gold nanorods can be routinely synthesized, within a wide range of sizes and aspect ratios, a similar level of control has not been reached for silver nanorods. Whereas seeded-growth processes have been developed, the reported methods have not met sufficient interest, mainly due to limited quality, in particular when small size (short diameter) and small aspect ratios are targeted. In the surfactant-driven seeded growth of gold nanorods, the success of the synthesis largely depends on the quality and stability of the seeds, and thus related methods have been reported for the seeded growth of Ag nanorods, using penta-twinned Au nanorods and bipyramids as seeds. However, Ag nanorods with diameters above 30 nm are consistently obtained, restricting their potential applications. We report the preparation of high quality silver nanorods, using either small bipyramids or small decahedra as seeds, with special attention to the location of the seeds, either at the center (bipyramids) or at one end (decahedra) of the resulting nanorods.

In spite of many efforts to discover less costly and more available materials, gold and silver are still the most commonly used plasmonic metals.[1] The main reasons behind the choice of such precious metals are their high charge carrier density and the relative simplicity of their chemistry, which allowed the development of a large amount of fabrication methods, yielding nanoparticles with tunable morphology and within a wide range of dimensions. Au is typically preferred because of its more noble character, i.e. higher chemical stability, which leads not only to more stable nanoparticles but also to more controlled crystal growth processes. A paradigmatic example is provided by nanorods. Since the pioneering work by Murphy and El-Sayed,[2] the surfactant-assisted seeded growth method has been improved essentially to perfection, for the particular case of gold.[3] For Ag however, most reported methods are either based on the use of organic solvents or result in poor quality and/or limited size tunability.

Ag nanorods and nanowires have been prepared by different methods,[4] including the thermal reshaping of Ag decahedra,[5] the polyol method,[6-9] light-assisted synthesis,[10,11] and seeded growth in water.[12-16] Some of these methods require the use of nanoparticle seeds made from different metals, like Au[7,12,13,15] or Pd,[6] which display high chemical stability and well-defined crystallographic facets. A general feature of such templated nanorods and nanowires is a penta-twinned crystallographic structure, comprising five {100} lateral facets and ten {111} facets at the tips.[5] It has been reported that {100} facets are favored for Ag, in the presence of chloride ions.[12] Therefore, both Au and Pd seeds with pentagonal symmetry have been preferred, including Pd decahedra,[6] Au nanorods[12,15] and nanobipyramids.[13,14,16] Although high monodispersity has been reported for the above referred methods, as well as a wide tunability of the aspect ratio, obtaining nanorods with diameters below 30 nm or with a small aspect ratio remains challenging.[17,18] Such small nanorods would be particularly preferred for applications where absorption should dominate over scattering, e.g. to exploit photothermal effects[19] or in optoacoustic imaging.[20]

The use of bipyramids as seeds for Ag nanorod growth is highly efficient, as reported by Zhuo et al.[14] This method requires the preparation of monodisperse bipyramids in high yields, which usually require extensive multistep processes including purification steps. Recent reports proposed the use of mild thermal ripening to largely increase the content of penta-twinned seeds, which in turn resulted in a major improvement in the yield and tunability of Au bipyramids.[21,22] We report herein the synthesis of Ag nanorods with narrow size distributions and wide tunability in aspect ratio (2.5 to 11), while keeping diameters below 30 nm. Although pentatwinned seeds from thermal ripening could not be directly used for Ag nanorod growth (see **Figure S1**), both small bipyramids and decahedra derived therefrom, served as templates to prepare high quality Ag nanorods, with similar dimensions but with an intriguing difference in the location of the seeds within the obtained nanorods.

Au bipyramids were prepared as recently reported[22] (see details in the Supporting Information, SI). The experimental conditions were selected to either grow small bipyramids (length: 35.7 ± 1.9 nm; width at center: 14.2 ± 0.5 nm; aspect ratio: 2.5 ± 0.1; see **Figure S2**) or decahedra with three different sizes

(11.7 ± 0.5, 15.2 ± 0.5, and 18.5 ± 0.5 nm; see **Figure S3**). Ag nanorods were then grown on Au bipyramids, in the presence of CTAC, by addition of $AgNO_3$ and ascorbic acid, at 60 ºC. Ag nanorods of different dimensions were prepared by simply increasing the $AgNO_3$ concentration in the growth solution (see **Table S1**), while keeping a constant [AA] : [Ag^+] molar ratio of 4. UV-Vis-NIR spectra for Ag nanorod dispersions obtained using different ratios between Ag^+ and Au bipyramid seeds, are displayed in **Figure 1**, clearly showing a gradual red-shift of the dipolar longitudinal localized surface plasmon resonance (LSPR), as the aspect ratio was increased. The narrow and symmetric LSPR bands, as well as the presence of higher order multipole bands for higher aspect ratios reflect a high monodispersity, as previously reported.[13,15] The high uniformity of the obtained nanorods is also clearly observed in the representative transmission electron microscopy images in **Figure 2**.

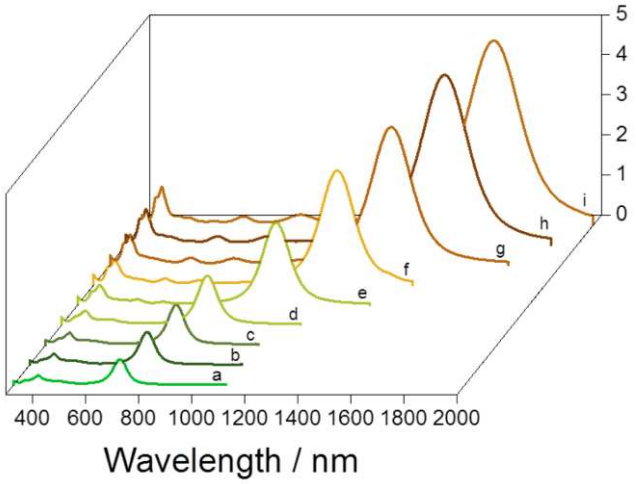

Figure 1. UV-Vis-NIR spectra of Ag nanorod dispersions grown from small Au bipyramids. The corresponding aspect ratios are 2.7 (a), 3.4 (b), 3.8 (c), 4.3 (d), 6.2 (e), 7.5 (f), 8.8 (g), 10.0 (h), and 10.9 (i), corresponding to maximum LSPR wavelengths between 700 and 1640 nm. The width was almost constant (17-20 nm), while the length was varied between 54 and 218 nm, through the growth conditions. Further details are provided in **Table S1**.

It should be noted that, whereas the length of the obtained nanorods increases linearly with the amount of added $AgNO_3$, the width remains constant (**Figure S4a**). As a consequence of the associated linear increase in aspect ratio, the LSPR position is linearly related to added Ag concentration, indicating the quantitative reduction of all added Ag^+ onto the existing bipyramid seeds (**Figure S4b**). Importantly, the diameters remain below 20 nm in all cases, well below previously reported Ag nanorods, usually above 30 nm in diameter.

A similar seeded growth process was used to synthesize Ag nanorods from decahedral Au seeds. In this case, as the seed diameter can be readily tuned by the mild growth conditions, we aimed at diameters between 10 and 20 nm. Three samples were prepared of decahedra with diameters of 12, 15 and 18 nm, and subsequently grown (keeping constant the concentration of Au^0) under identical experimental conditions. The results, which are summarized in **Table S2** and **Figure S5**, confirm that the seed size determines the diameter of the resulting nanorods, whereas the length is determined by the amount of Ag reduced on each seed. Indeed, for a constant molar amount of Au, the amount of seed nanoparticles is larger for a smaller particle size, resulting in smaller grown Ag nanorods. For the selected conditions, nanorods with increasing aspect ratio result from growth on larger seeds (**Table S2**), with a corresponding red-shifted LSPR (**Figure S5a**).

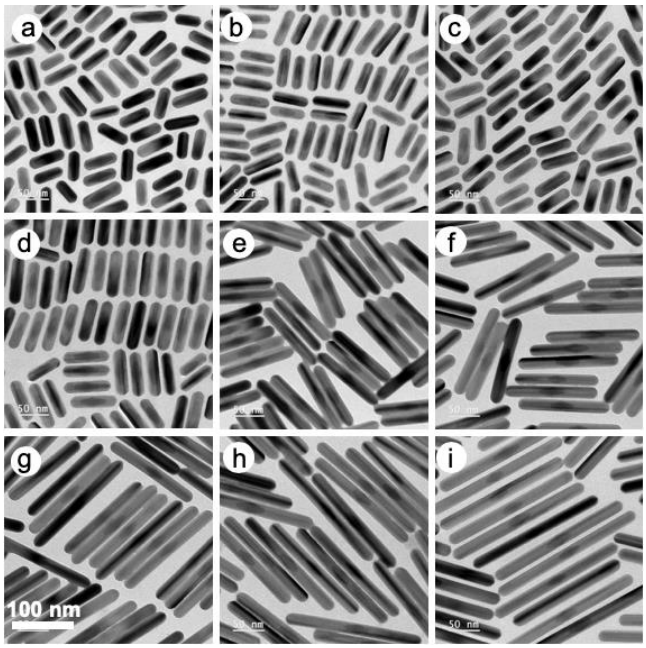

Figure 2. Representative TEM images of Ag nanorods with the optical spectra presented in Figure 1.

The TEM images in **Figures 2 and S5** show a seemingly identical appearance for Ag nanorods grown from bipyramids and from decahedra, in both cases maintaining a thickness dictated by the equatorial axis of the seeds and with a morphological yield close to unity. However, upon closer inspection of the images, we found an interesting difference in the location of the seeds. Whereas bipyramid seeds show a general tendency to be located at the center of the nanorod (**Figure 2**), in the case of decahedra (**Figure S5**), we observe that the seeds are mostly placed near / at one of the tips (see a higher magnification image in **Figure S5e**). Although it is far from straightforward to propose a general mechanism that would account for such striking differences, further discussion should involve relevant differences between bipyramids and decahedra, in connection with further Ag growth. We do note a major difference in the synthesis of Au seeds, related to the addition of $AgNO_3$. Whereas Ag^+ ions are required for the growth of high quality bipyramids, the formation of decahedral seeds is Ag-free. Related effects can also be found in the literature, where the use of (Ag-containing) Au nanorods[15] or larger bipyramids[13,14] typically leads to Ag nanorods/nanowires with the seed located at the center, but nanorods with the seed located at one tip were grown from (Ag-free) Pd decahedral seeds.[6] A word of caution should however be given here, as the latter work involved the use of high temperature (200 ºC) and different solvent (ethylene glycol) and stabilizer (poly(diallyldimethylammonium)chloride), meaning that the mechanism is likely dictated by different parameters and therefore a direct comparison might be easily flawed.

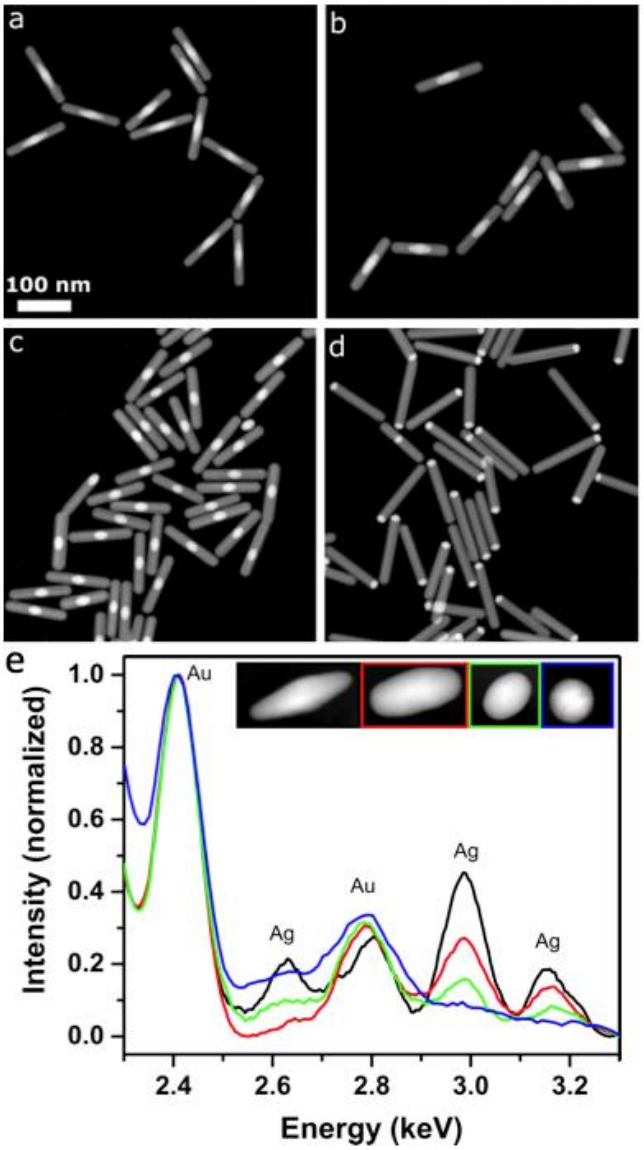

Figure 3. HAADF-STEM images of Ag@Au NRs grown from bipyramids (a), etched bipyramids (b, c) and decahedra (d). (e) EDX spectra of the corresponding seeds in the energy region of the Ag $L\alpha_1$ and $L\beta_1$ peaks.

We tested this argument through additional experiments, in which Au bipyramids were gradually etched by Au(III) in the presence of cetyl-trimethylammonium bromide (CTAB)[23] (see **Figures S6-S8** and **Table S3**). As a result, the anisotropy of Ag-containing seeds was gradually reduced, so that they would be morphologically more similar to decahedra. A summary of the results obtained for the growth of Ag nanorods from three etching steps and Au decahedra is provided by high angle annular dark field scanning transmission electron microscopy (HAADF-STEM) images (**Figure 3**). Energy dispersed X-ray (EDX) elemental analysis of the so-prepared seeds confirmed the presence of Ag (preferentially near the surface) on the initial and etched bipyramids, but no Ag in the decahedral seeds (**Figures 3e and S9**). Since the contrast depends on the atomic number Z, the Au seeds can be readily identified within Ag nanorods. From these images (additional TEM and UV-Vis spectroscopy data are shown in **Figures S6-S8**) it is clear that the seeds are preferentially located at the center when they contain Ag (bipyramids and etched bipyramids, **Figure 3a-c**) but they remain at one tip when grown from (Ag-free) decahedra (**Figure 3d**).

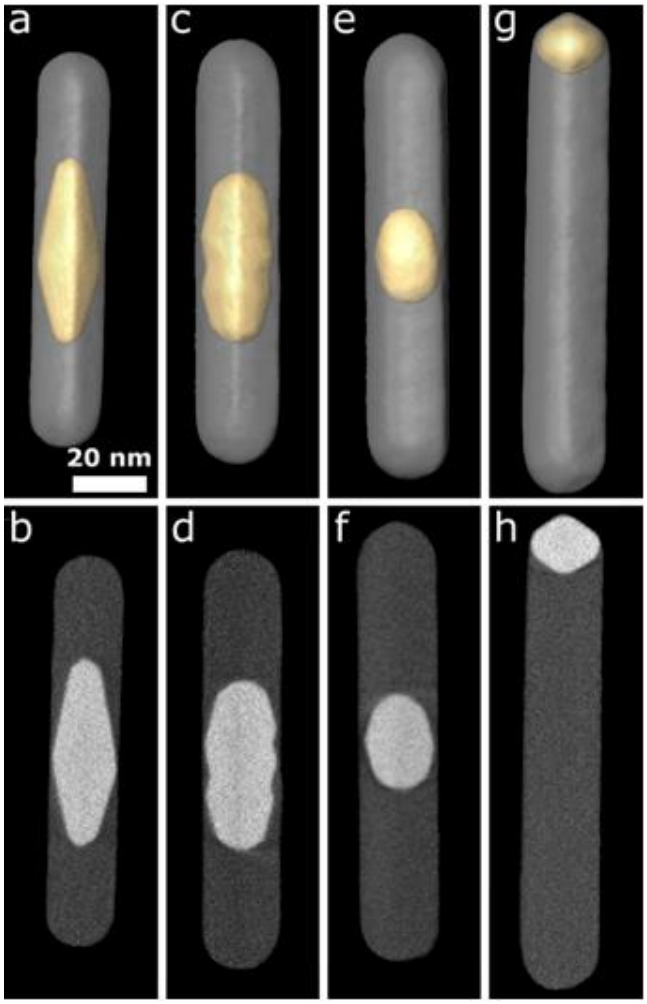

Figure 4. Electron tomography analysis of Ag nanorods grown from: as prepared Au bipyramid seeds (a,b), mildly etched bipyramids (c,d), strongly etched bipyramids (e,f), and decahedral Au seeds (g, h). Au cores are readily distinguished because of its higher electron density.

We additionally carried out a more detailed 3-dimensional study of the morphology of the resulting nanoparticles, combining HAADF-STEM and tomography. The difference in electron density between Au and Ag allowed us not only to obtain a detailed description of the overall morphology but also to identify the location and relative orientation between Au cores and Ag shells. Representative examples of Ag rods grown from Au bipyramids, etched bipyramids and decahedra, are shown in **Figure 4**. These images clearly show that Au bipyramid etching gradually reduced the anisotropy, into less perfect morphologies than the initial bipyramids. However, in all cases bipyramid-derived seeds are located at the longitudinal center of the nanorods, whereas decahedral seeds are well-oriented at the very tip. Interestingly, all obtained Ag nanorods retained a pentagonal cross-section, as clearly confirmed by the corresponding animated reconstructions (**Movies S1-S4**). Detailed cross-sectional views (**Figure S10**) further confirm that Ag nanorods retain the pentagonal cross section from the inner seeds. The

presence of twins and the expected epitaxial growth of Ag on Au seeds was additionally confirmed by high resolution STEM (**Figure S11**), where it can also be observed that only a few atomic layers of Ag have grown on the tip side of the decahedral seed and on the equatorial plane of the bipyramid seed. Epitaxial growth, as shown in Figure S11, is not surprising, considering that the lattice constants of Au (4.079 Å) and Ag (4.085 Å) are very similar. It has been reported that, for systems with a larger mismatch in lattice parameter, such as Au and Pd, the seed position might be affected.[24] Although it is not straightforward to obtain a 3D visualization of the twinning configuration for the NRs in this study, Figures S10 and S11 are in good agreement with the presumed pentatwinned structure. Previous 3D characterization of similar structures indicated that the presence of twins in the seeds extends over the entire overgrown structure.[25] This is also confirmed by the atomic resolution contrast in Figure S11.

Further evidence supporting the proposed mechanism is provided by an additional control experiment. The same Au decahedral seeds used for the sample shown in Figure 3d were incubated overnight at 30 ºC with silver ions, and subsequently a reduction step was performed under similar conditions as described in the Experimental section (SI). TEM analysis evidenced that the decahedral seeds were located at the end of rods. However, if a thin Ag layer is first deposited on the same gold decahedra (EDX analysis reveals that Ag content is ca. 9 at%, see **Figure S12**) and then silver growth is carried out under the same conditions, the resulting nanorods were found to contain both seeds at the center and close to one tip (**Figure S13**).

In addition, we performed a kinetic analysis of Ag reduction on etched bipyramids and decahedra with similar dimensions. The results (**Figure 5**) clearly indicate that Ag deposition rate on Au decahedra is slower than that on etched bipyramids. We conclude that the presence of Ag in the seeds may have a catalytic effect, whereas Ag-free Au decahedra need an induction time (see Figure 5c) for initial Ag deposition. This kinetic barrier may be responsible for the asymmetric growth of Ag nanorods on decahedral seeds. It should also be noted that bipyramids exhibit high-index facets (higher surface energy) while decahedra are bound by low-index facets (111) (lower surface energy). Faster Ag growth can be expected on high surface energy facets (bipyramids), equally from both sides, resulting in nanorods with seeds located at the center. On the other hand, slower Ag reduction kinetics on the lower surface energy decahedra may influence the preferential growth from one side upon Ag deposition.

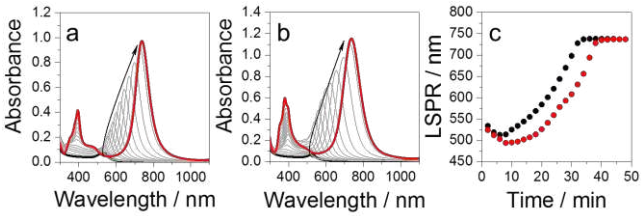

Figure 5. a,b) UV-Vis-NIR spectral evolution during the formation of Ag nanorods, after addition of silver precursor and ascorbic acid at 60 ºC, from etched bipyramids (a) and gold decahedra (b). c) Time trace of the longitudinal LSPR band during Ag reduction.

In summary, we implemented a seeded-growth method to grow small Ag nanorods with diameters below 20 nm, featuring high monodispersity, wide tunability in aspect ratio and LSPR wavelength tunability, from the visible well into the NIR. Although the use of both Au bipyramids and Au decahedra lead to Ag nanorods with similar quality, a remarkable difference was observed in the growth mechanism, resulting in the original seeds being located either in the center or at one of the tips. Such a difference in growth mechanism appears to correlate with the presence of Ag in the seed composition.

ASSOCIATED CONTENT

Supporting Information

Experimental details, list of Ag nanorod dimensions, additional UV-vis spectra and TEM images, EDX elemental mapping of seeds, selected HRTEM images (PDF).
Movies showing electron tomography reconstructions of selected Ag nanorods (MP4).

The Supporting Information is available free of charge on the ACS Publications website.

AUTHOR INFORMATION

Corresponding Author

* Luis M. Liz-Marzán
e-mail: llizmarzan@cicbiomagune.es

Author Contributions

A. Sánchez-Iglesias and X. Zhuo synthesized nanorods, W. Albrecht carried out high-end electron microscopy characterization, which was analyzed together with S. Bals. L.M. Liz-Marzán supervised the work and participated in data discussion and interpretation. The manuscript was written through contributions of all authors. All authors have given approval to the final version of the manuscript.

ACKNOWLEDGMENT

Financial support is acknowledged from the European Commission under the Horizon 2020 Programme by means of the grant agreement No. 731019 (EUSMI), the ERC Consolidator Grant No. 815128 (REALNANO) and the ERC Advanced Grant No. 787510 (4DbioSERS). WA acknowledges an Individual Fellowship from the Marie Sklodowska-Curie actions (MSCA) under the EU's Horizon 2020 program (Grant 797153, SOPMEN). This work was performed under the Maria de Maeztu Units of Excellence Program from the Spanish State Research Agency – Grant No. MDM-2017-0720.

REFERENCES

1. Liz-Marzán, L. M.; Murphy, C. J.; Wang, J. Nanoplasmonics. *Chem. Soc. Rev.* **2014**, *43*, 3820–3822.
2. Lohse, S. E.; Murphy, C. J. The Quest for Shape Control: A History of Gold Nanorod Synthesis. *Chem. Mater.* **2013**, *25*, 1250–1261.
3. Scarabelli, L.; Sánchez-Iglesias, A.; Pérez-Juste, J.; Liz-Marzán, L. M. A "tips ´n tricks" Practical Guide to the Synthesis of Gold Nanorods. *J. Phys. Chem. Lett.* **2015**, *6*, 4270–4279.
4. Rycenga, M.; Cobley, C. M.; Zeng, J.; Li, W. Y.; Moran, C. H.; Zhang, Q.; Qin, D., Xia, Y. Controlling the Synthesis and Assembly of Silver Nanostructures for Plasmonic Applications. *Chem. Rev*. **2011**, *111*, 3669–3712
5. Pietrobon, B.; McEachran, M.; Kitaev, V. Synthesis of Size-Controlled Faceted Pentagonal Silver Nanorods with Tunable Plasmonic Properties and Self- Assembly of These Nanorods. *ACS Nano* **2009**, *3*, 21–26.

6. Luo, M.; Huang, H.; Choi, S.-I.; Zhang, C.; da Silva, R. R.; Peng, H.-C.; Li, Z.-Y.; Liu, J.; He, Z.; Xia, Y. Facile Synthesis of Ag Nanorods with No Plasmon Resonance Peak in the Visible Region by Using Pd Decahedra of 16 nm in Size as Seeds. *ACS Nano* **2015**, *9*, 10523–10532.
7. Tsuji, M.; Matsumoto, K.; Miyamae, N.; Tsuji, T.; Zhang, X. Rapid Preparation of Silver Nanorods and Nanowires by a Microwave-Polyol Method in the Presence of Pt Catalyst and Polyvinylpyrrolidone. *Cryst. Growth Design* **2007**, *7*, 311–320.
8. Patarroyo, J.; Genç, A.; Arbiol, J.; Bastús, N. G.; Puntes, V. One-Pot Polyol Synthesis of Highly Monodisperse Short Green Silver Nanorods. *Chem. Commun*. **2016**, *52*, 10960–10963.
9. Yang, Y.; Wang, W.; Li, X.; Chen, W.; Fan. N.; Zou, C.; Chen, X.; Xu, X.; Zhang, L.; Huang, S. Controlled Growth of Ag/Au Bimetallic Nanorods through Kinetics Control. *Chem. Mater.* **2013**, *25*, 34−41.
10. Zhang, J.; Langille, M. R.; Mirkin, C. A. Synthesis of Silver Nanorods by Low Energy Excitation of Spherical Plasmonic Seeds. *Nano Lett.* **2011**, *11*, 2495–2498.
11. Langille, M. R.; Personick, M. L.; Mirkin, C. A. Plasmon-Mediated Syntheses of Metallic Nanostructures. *Angew. Chem., Int. Ed*. **2013**, *52*, 13910–13940
12. Gómez-Graña, S.; Goris, B.; Altantzis, T.; Fernández-López, C.; Carbó-Argibay, E.; Guerrero-Martínez, A.; Almora-Barrios, N.; López, N.; Pastoriza-Santos, I.; Pérez-Juste, J.; Bals, S.; Van Tendeloo, G.; Liz-Marzán, L. M. Au@Ag Nanoparticles: Halides Stabilize {100} Facets. *J. Phys. Chem. Lett.* **2013**, *4*, 2209–2216.
13. Li, Q.; Zhuo, X.; Li, S.; Ruan, Q.; Xu, Q-H.; Wang, J. Production of Monodispersed Gold Nanobipyramids with Number Percentages Approaching 100% and Evaluation of Their Plasmonics Properties. *Adv. Opt. Mater.* **2015**, *3*, 801–812.
14. Zhuo, X.; Zhu, X.; Li, Q.; Yang, Z.; Wang, J. Gold Nanobipyramid-Directed Growth of Length-Variable Silver Nanorods with Multipolar Plasmon Resonances. *ACS Nano* **2015**, *9*, 7523–7535.
15. Mayer, M.; Scarabelli, L.; March, K.; Altantzis, T.; Tebbe, M.; Kociak, M.; Bals, S.; García de Abajo, F. J.; Fery, A.; Liz-Marzán, L. M. Controlled Living Nanowire Growth: Precise Control over the Morphology and Optical Properties of AgAuAg Bimetallic Nanowires. *Nano Lett.* **2015**, *15*, 5427–5437.
16. Zhu, X.; Zhuo, X.; Li, Q.; Yang, Z.; Wang, J. Gold Nanobipyramid-Supported Silver Nanostructures with Narrow Plasmon Linewidths and Improved Chemical Stability. *Adv. Funct. Mater.* **2016**, *26*, 341–352.
17. Xia, Y.; Xiong, Y.; Lim, B.; Skrabalak, S. E. Shape-Controlled Synthesis of Metal Nanocrystals: Simple Chemistry Meets Complex Physics? *Angew. Chem. Int. Ed.* **2009**, *48*, 60–103.
18. Zhu, J.; Zhang, G.; Chang, W.; Luan, X.; Qu, F.; Zheng, Y. Facile Synthesis of Silver Nanorods/Nanowires with Sub-20 Nm Diameter and Their Trimetallic Hollow Derivatives Using Tiny Au Seeds. *Mater. Lett.* **2020**, *272*, 127804.
19. Maestro, L. M.; Haro-González, P.; Sánchez-Iglesias, A.; Liz-Marzán, L. M.; Solé, J. G.; Jaque, D. Quantum Dot Thermometry Evaluation of Geometry Dependent Heating Efficiency in Gold Nanoparticles. *Langmuir* **2014**, *30*, 1650–1658.
20. Chen, Y.-S.; Zhao, Y.; Yoon, S. J.; Gambhir , S. S.; Emelianov. S. Miniature Gold Nanorods for Photoacoustic Molecular Imaging in the Second Near-Infrared Optical Window. Nat Nanotechnol. **2019**, *14*, 465-472.
21. Chateau, D.; Liotta, A.; Vadcard, F.; Navarro, J. R. G.; Chaput, F.; Lermé, J.; Lerouge, F.; Parola, S. From Gold Nanobipyramids to Nanojavelins for a Precise Tuning of the Plasmon Resonance to the Infrared Wavelengths: Experimental and Theoretical Aspects. *Nanoscale* **2015**, *7*, 1934–1943.
22. Sánchez-Iglesias, A.; Winckelmans, N.; Altantzis, T.; Bals, S.; Grzelczak, M.; Liz-Marzán, L. M. High-Yield Seeded Growth of Monodisperse Pentatwinned Gold Nanoparticles through Thermally Induced Seed Twinning. *J. Am. Chem. Soc.* **2017**, *139*, 107−110.
23. Rodríguez-Fernández, J.; Pérez-Juste, J.; Mulvaney P.; Liz-Marzán, L. M. Spatially-Directed Oxidation of Gold Nanoparticles by Au(III)-CTAB Complexes. *J. Phys. Chem. B* **2005**, *109*, 14257–14261.
24. Winckelmans, N.; Altantzis, T.; Grzelczak, M.; Sánchez-Iglesias, A.; Liz-Marzán, L. M.; Bals S. Multimode Electron Tomography as a Tool to Characterize the Internal Structure and Morphology of Gold Nanoparticles. *J. Phys. Chem. C* **2018**, *122*, 13522-13528.
25. Smith J. D.; Bladt E.; Burkhart J. A. C.; Winckelmans, N.; Koczkur, K. M.; Ashberry, H. M.; Bals, S.; Skrabalak, S. E.; Defect-Directed Growth of Symmetrically Branched Metal Nanocrystals. *Angew. Chem. Int. Ed.* **2020**, *59*, 943-950.

TOC graphic: